Mathematical Modeling of Heat and Mass Transfer in Packed-Bed Adsorbers/Regenerators

G. S. Gouvalias and N. C. Markatos
Dept. of Chemical Engineering, National Technical University of Athens, Athens, Greece

Nonisothermal adsorption is studied by incorporating its mathematical description into a model consisting of the full two-dimensional Navier-Stokes equations and energy and species concentration equations to simulate the processes in fixed-bed industrial adsorbers/regenerators. The model partial-differential equations are solved numerically by using well-established computational fluid dynamics techniques. The equilibrium between gas and solid is considered nonlinear, which is described by Freundlich-type equations. The transport and adsorption of a compound from a solvent to and into an adsorbent are described by a two-step process: transport through the "film" to the outer surface of the particle and diffusion into the porous particle. The effect of fill resistance is discussed, as well as a two-equation turbulence model. Solutions obtained for a typical industrial adsorber/regenerator demonstrate the potential of this method. The computed results for various flow ratios and parameters in the Freundlich equations are shown to be physically plausible.

Introduction

Adsorber-regenerators are used extensively in the process industries for gas cleaning and separation. In the field of gaseous separations, adsorption is used to dehumidify air and other gases, to remove objectionable odors and impurities from industrial gases such as CO_2, to recover valuable solvent vapors from dilute mixtures with air and other gases, and to fractionate mixtures of hydrocarbon gases containing substances such as methane, ethylene, ethane, propylene and propane.

The fixed bed of adsorbent beads is supported within a vertical cylinder with a baffle installed to ensure satisfactory flow distribution. Gas is pumped through the bed, which selectively removes certain components. Bad flow distributions can lead to poor product quality, loss of feedstock and excessive energy use. When the beads are nearly saturated, the sorbate is recovered from them by a change in the operating conditions. There may be, for example, a decrease in pressure (pressure-swing adsorption) or an increase in temperature (temperature-swing adsorption).

Adsorbents are necessarily porous solids and the porosity plays an essential role in determining the way in which gases or vapors are adsorbed under various conditions of concentration, temperature, and so on. It, however, is not necessarily the most porous adsorbent which adsorbs the most gas. The structure of the pores, their size, uniformity and arrangement must also be taken into account.

Chemical processes introduce a further level of complexity, requiring means of evaluating the relevant heat- and mass-transfer rates, (Perry and Chilton, 1973). Typical applications include the removal of the air from natural gas prior to cryogenic processing. Pressure-swing adsorption is seen as a future alternative to distillation, in the preparation of intermediate amounts of low quality oxygen.

Breakthrough curves for experiments described in, for example, Marcussen (1982) are predicted by means of different models for adsorption in integral fixed beds.

First, the breakthrough time is predicted by some models assuming isothermal adsorption. The method described by Treybal (1968) is based on the assumptions of a constant-pattern mass-transfer zone and an overall driving force for the transfer of adsorbate from the flowing fluid to the adsorbent. The model of Hougen (1948) considers mass transfer controlled by gas-film resistances and describes the adsorption equilibrium by a linear relationship. Kyte (1973) also assumes film controlled mass transfer, but allows for a nonlinear adsorption equilibrium by using a Freundlich isotherm. Rosen (1954) maintains Hougen's assumption of the linear adsorption equilibrium, but includes a diffusion resistance within the adsorbent in addition to the fluid film resistance.

Work on nonisothermal adsorption in packed beds has been reported, for example, by Meyer and Weber (1967); but their

Table 1. Review of Adsorption Model

Diffusion Model	Equilibrium	Adsorbate Phase	System	Film Resistance	Math. Treatment
HS	LI	G	Bed	Yes	A
HS	LI	G	Bed	No	A
P	LI	G	Batch	No	A
P	LI	G	Bed	Yes	A
P	NL	G	Bed	Yes	N

HS = homogeneous solid; P = pore; LI = linear adsorption; NL = nonlinear adsorption; G = gas; A = analytical solution; N = numerical solution.

solutions are given for parameter values different from those in the experiments mentioned above. The method for nonisothermal adsorption, which is further developed by Pan and Basmadjian (1970), assumes the existence of two constant-pattern transfer zones separated by an equilibrium zone; mass transfer from gas to adsorbent being described by an overall transfer coefficient.

Most of the existing adsorption models have been based on restrictive assumptions, such as no film resistance between the solution and adsorbent, and linear equilibrium between the solute and adsorbent.

After careful consideration of the assumptions made in each of the models presented in Table 1, the ones proposed by Mckay (1984) have been selected for developing the adsorption model reported in this article, since they appear to respond best to reality.

The homogeneous solid-phase diffusion model is used to represent the rate of adsorption of a solute from the gas phase to the solid adsorbent. The mechanistic processes involved are film diffusion from the gas phase to the solid phase, equilibrium adsorption on the surface, and unsteady-state internal transport to the center of the adsorbent particle. Weber and Chakravorti (1974) have provided detailed descriptions of the procedure for estimating the adsorption-rate parameters, that is, the film mass-transfer coefficient and the surface-diffusion coefficient.

The objective of the present work is to develop a mathematical model for nonisothermal adsorption and incorporate it into more general computational fluid dynamics (CFD) models that predict flow, temperature and concentration fields. CFD is now an important tool for the design and development of equipment and processes in the fields of mechanical, nuclear and aeronautical engineering. It has great potential for application in the process industry, where many key issues in design are related to the behavior of fluids in turbulent flow, often involving more than one phase, reaction and heat transfer. The present state of the art in CFD is such that there is a need for extensive evaluation of CFD models before they can be used for design. This work is the first step in this direction for the processes of adsorption/regeneration. A lot of research remains to be done with the present model in order to improve and validate its submodels of such physical processes as particles-wall interaction, porosity, and so on. The proposed mathematical model for nonisothermal adsorption in industrial adsorbers/regenerators is described below.

Theoretical Model

Physical model and nature of the analysis

The physical problem concerns the fluid flow and transport of heat and mass in a two-dimensional, cylindrical, axisymmetrical adsorber/regenerator. During the adsorption stage, process air is blown up through the lower inlet of a cylindrical vessel; it flows up through the packed bed which is fixed inside the vessel and leaves through an upper pipe. The trace impurities are adsorbed into the molecular sieves. When the beads approach their equilibrium loading of trace impurities, it is necessary to change the operating conditions in order to remove the trace impurities from the beads (regeneration stage). This is done by blowing hot air down through the bed for a limited time period. The use of the bed can then be switched back to the adsorption cycle.

The present analysis is based on the numerical solution of the set of the full partial-differential equations that express the physical phenomena occurring in the vessel during operation. They are mathematical expressions of the conservation principle for mass, momentum, energy and chemical species in transient, two-dimensional recirculating flows.

To solve the equations, the domain of interest is discretized with a finite-difference grid into a number of finite volumes and the differential equations are integrated over these volumes. The resulting "finite-domain" equations are solved by efficient linear solvers. Suitable assumptions are made about the physical processes involved, and the appropriate boundary and initial conditions are fitted into a computer model which is incorporated into a general CFD program environment. Computer runs of the resulting model are made and their primary results are the grid-node values of the two velocity components (axial and radial), pressure, temperature and concentration, at each time step.

Independent and dependent variables

The independent variables of the problem are the two components of a cylindrical polar coordinate system, (z, r), and time, t.

The dependent variables (time-average values) of the problem are the two velocity components w, v, in the z and r directions (m/s), respectively; the pressure p (N/m^2); the adsorbate concentration in the gas phase C_g (kg/kg fluid); the adsorbate concentration in the solid phase, C_p, $-$(kg/kg), at the gas-solid interface in equilibrium with C_g; the concentration of adsorbate inside the pellet C_s (kg/kg); the gas-phase temperature T_g (K); the particle-surface temperature T_s (K); and two characteristics of gas turbulence, namely the turbulence kinetic energy k (m^2/s^2), and its dissipation rate, ϵ (m^3/s^2).

Partial-differential equations

The time-dependent equations for continuity, velocity components, temperature and chemical species concentration are given below.

Continuity. The pressure variable is associated with the continuity equation:

$$\frac{\partial \rho}{\partial t} + \text{div}(\rho \vec{v}) = 0 \tag{1}$$

in anticipation of the so-called pressure-correction equation (Patankar and Spalding, 1972), which is deduced from the finite-difference form of the continuity equation. In the above equation, ρ is density and $\vec{v}$ is the velocity vector.

Momentum Equations. In cylindrical polar coordinates, the unsteady-state equations of motion may be conveniently presented in the following two-dimensional form with axial and radial coordinates z and r, respectively,

For the z-direction momentum:

$$\frac{\partial}{\partial t}(\rho w)+\frac{1}{r}\cdot\left[\frac{\partial}{\partial z}(r\rho w\cdot w)+\frac{\partial}{\partial r}(r\rho v\cdot w)\right]$$
$$=\underbrace{-\frac{\partial p}{\partial z}+\frac{\partial}{\partial z}\left(\mu_{\text{eff}}\frac{\partial w}{\partial z}\right)+\frac{1}{r}\frac{\partial}{\partial r}\left(r\mu_{\text{eff}}\frac{\partial v}{\partial z}\right)-F_w-S_{w,P}-S_w-S_{\text{Ergun},w}}_{S_w} \quad (2)$$

For the r-direction momentum:

$$\frac{\partial}{\partial t}(\rho v)+\frac{1}{\mathrm{r}}\cdot\left[\frac{\partial}{\partial z}(r\rho w\cdot v)+\frac{\partial}{\partial r}(r\rho v\cdot v)\right]$$
$$=\underbrace{-\frac{\partial p}{\partial r}+\frac{\partial}{\partial z}\left(\mu_{\text{eff}}\frac{\partial w}{\partial r}\right)+\frac{1}{r}\frac{\partial}{\partial r}\left(r\mu_{\text{eff}}\frac{\partial v}{\partial r}\right)-\frac{2\mu_{\text{eff}}v}{r^2}-F_v-S_{v,P}-S_v-S_{\text{Ergun},v}}_{S_v} \quad (3)$$

where w, v are the axial and radial velocity components, respectively; μ_{eff} is the effective viscosity and S_Φ represents the source/sink terms. The source/sink term S_Φ for the momentum equations contain contributions such as: pressure gradient, viscous force exerted on gas phase by stresses within that phase, wall friction (F_Φ), momentum loss at the surfaces of the vessel ($S_{\Phi,P}$), momentum loss at perforated screens (S_Φ) and momentum loss in the packed bed (Ergun equation, $S_{\text{Ergun},\Phi}$).

Gas-Phase Adsorbate Concentration Equation. A mass balance on the gas phase gives:

$$\rho_f\cdot\frac{\partial C_g}{\partial t}=\nabla D_{\text{eff}}\nabla C_g-\nabla\vec{v}C_g$$
$$+3\cdot\rho_f\cdot(1-\epsilon_f)\cdot\frac{k_f}{\epsilon_f r_p}\cdot(C_p|_{r=r_p}-C_g) \quad (4)$$

where ϵ_f is the void fraction of the bed; D_{eff} is the effective diffusivity in the gas phase (m^2/s); r_p is the particle radius, (m); k_f, is the mass-exchange coefficient at pellet surface; and ρ_f is the gas density. The first term of Eq. 4 corresponds to accumulation, the second to diffusion, the third to convection and the fourth to sources.

Nonlinear Freundlich Isotherm

$$C_p=k(T)\cdot C_g^\beta \quad (5)$$

is used to describe the adsorption equilibrium, where, C_g (kg/kg fluid) is the adsorbate concentration in the gas phase and C_p (kg/kg) is adsorbate concentration in the solid phase, at the gas-solid interface in equilibrium with C_g. The constant $k(T)$ is a function of temperature (T), whereas β is taken to be constant. The heat of adsorption q_{st} is related to $k(T)$ for each gas by Van't Hoff's equation:

$$\frac{k}{T}=\left(\frac{k}{T}\right)_{1/T\to 0}\exp\left(\frac{q_{st}}{R_gT}\right) \quad (6)$$

Most correlations that relate the gas mass-transfer coefficient, k_f to the other system parameters use the Colburn-Chilton (Upadhyay and Tripathi, 1975) mass-transfer factor j_D, defined as:

$$j_D=\frac{k_f}{u_s}\cdot N_{Sc}^{2/3},\qquad N_{Sc}=\left(\frac{\mu_f}{\rho_f\cdot D_{AB}}\right) \quad (7)$$

where u_s is the superficial fluid velocity, (m/s); and N_{Sc} is the Schmidt number of the flowing gas, that is, the ratio of the gas kinematic viscosity to the gas-phase diffusivity, D_{AB}, of the solvent in the gas, (m^2/s).

The following well-established relation, for different temperatures and different pressures, was used to estimate the gas-phase diffusivity:

$$D_{AB}=D_{AB,0}\cdot\frac{P_1}{P_2}\left(\frac{T_2}{T_1}\right)^{3/2} \quad (8)$$

where $D_{AB,0}$ is the gas-phase diffusivity at 273 K temperature and 1 atm pressure.

Several correlations are available relating the Colburn-Chilton factor, j_D, to the superficial linear velocity in packed beds of particles (Upadhyay and Tripathi, 1975). The most recent correlation, derived by Hsieng and Thodos (Dwivedi and Upadhyay, 1977), takes the form:

$$j_D=\frac{0.48}{\epsilon_f\cdot(N_{Re})^{0.39}} \quad (9)$$

where ϵ_f is the void volume fraction in the adsorber (bed), and N_{Re} is the Reynolds number of the flowing fluid, defined as:

$$N_{Re}=\frac{d_p\cdot u_s\cdot\rho_f}{\mu_f\cdot\varphi\cdot\alpha_f} \quad (10)$$

where d_p is the mean particle diameter in the bed, (m); and φ is the shape factor (φ = 1, for spherical particles).

Solid-Phase Adsorbate Concentration Equation. To describe mass transfer within the adsorbent particles the following assumptions are made:

• The surface maintains a rapid thermodynamic equilibrium with the fluid.

• $D_{\text{pore},i}$, the pore diffusivity (m^2/s), applies to movement within the macropores of the pellet, and therefore it has a value orders of magnitude less than that in the fluid phase.

The above assumptions appear from the literature to response to reality.

The adsorption rate is considered to be governed by the solid-phase mass-transfer processes. The rate of change of concentration within the bed is:

$$\frac{\partial C_s}{\partial t} = \{k_i(D_{\text{pore},i})\} \cdot \Psi_p \cdot \alpha_f \cdot (C_p - C_s) \tag{11}$$

where C_s is the concentration of the adsorbed phase inside the particles, (kg/kg) and k_i is the mass-transfer coefficient inside the particles (1/s).

The product $k_i \cdot \alpha_f$ is related to diffusivity and to effective spherical particle diameter d_p through the equation:

$$k_i \cdot \alpha_f = \frac{60 \cdot D_{\text{pore}}}{d_p^2} \tag{12}$$

The specific surface per unit volume of adsorber particle, α_f, is a function of the adsorbent particle size, d_p, and of the volumetric void fraction of the adsorbent bed. For spherical particles, and for cylindrical pellets with a length equal to the diameter, an assumption that facilitates the analysis, it is given by:

$$\alpha_f = \frac{6 \cdot (1 - \epsilon_f)}{d_p} \tag{13}$$

Hence, $k_i = 10 D_p/(d_p(1-\epsilon))$; the factor $(1-\epsilon)^{-1}$ entering because the solid concentration per unit particle volume is higher than that per unit bed volume. The factor $\psi_p \approx 1$ is obtained by comparing the true slope of the time curve of particle uptakes, as in a packed-bed (Perry and Chilton, 1973), with that given by Eq. 11 at $Y = 0.5$ (where Y is the dimensionless concentration).

Conservation of Energy Equation. The model of the present work, which we shall call the extended computational packed-bed model (ECOPAM), is developed under the assumptions that temperature inside the particles is uniform, the bed is adiabatic, the particles are spherical or cylindrical (with length equal to diameter) and the solid properties are constant over the temperature range of interest.

Then, an energy balance for the gas phase and one around a solid particle lead to the following equations.

For the gas phase:

$$\rho_f C_p \frac{\partial T_g}{\partial t} = \vec{\nabla} \cdot k_L \vec{\nabla} T_g - \rho_f C_p \vec{\nabla} \vec{v} T_g \underbrace{- \left(\frac{1-\epsilon}{\epsilon}\right) \frac{3h}{r_p} (T_g - T_s|_{r=r_p})}_{S_\Phi} \tag{14}$$

For the solid phase:

$$\rho_p C_p \frac{\partial T_s}{\partial t} = \underbrace{h \cdot \frac{6(1-\epsilon_p)}{d_p} (T_g - T_s) + k_i \lambda_{\text{ad}} (C_p - C_s)}_{S_\Phi} \tag{15}$$

where h is the gas-solid heat-transfer coefficient, ϵ_p is particle void fraction and λ_{ad} is the heat of adsorption.

The "local" heat-transfer coefficient is given by:

$$h = \frac{j_h C_p V \cdot \epsilon_p}{(Pr)^{2/3}_{\text{film}}} \tag{16}$$

where *film* denotes conditions at the "film" temperature, C_p is the specific heat of the phase in question, and V is the velocity inside the bed. The j_h factor is given by a Colburn factor formula as function of the Reynolds number.

The final expression relating the heat-transfer coefficient to velocity and particle size for "uniform" mixtures was found to be (SeeSee and Thomson, 1977):

$$h = \frac{0.289 G^{0.54}}{6(1-\epsilon_p)} \tag{17}$$

where G is the mass flow superficial velocity, that is, $G = \rho V \epsilon_p$. Equation 17 is estimated to be accurate to within $\pm 10\%$, approximately.

Turbulence Model (k-ϵ Model). The standard ($k \sim \epsilon$) model of turbulence (Launder and Spalding, 1974; Spalding, 1980a) is used outside the bed, and a constant turbulence viscosity is specified inside the bed for the gaseous phase. This model involves two transport equations for the turbulence characteristics. One governs the distribution through the field of k, the local kinetic energy of the fluctuating motion; the other governs a turbulence characteristic of different dimensions, namely ϵ, the energy dissipation rate (first proposed by Harlow and Nakayama, 1968).

For the transport equation for k:

$$\frac{\partial}{\partial t}(\rho k) + \frac{1}{r} \cdot \left[\frac{\partial}{\partial z}(r \rho w k) + \frac{\partial}{\partial r}(r \rho v k)\right] - \frac{1}{r} \cdot \left[\frac{\partial}{\partial z}\left(r \cdot \frac{\mu_{\text{eff}}}{\sigma_{k,\text{eff}}} \cdot \frac{\partial k}{\partial z}\right)\right] - \frac{1}{r}\left[\frac{\partial}{\partial r}\left(r \cdot \frac{\mu_{\text{eff}}}{\sigma_{k,\text{eff}}} \cdot \frac{\partial k}{\partial r}\right)\right] = \underbrace{\mu_t \left\{2\left[\left(\frac{\partial w}{\partial z}\right)^2 + \left(\frac{\partial v}{\partial r}\right)^2 + \left(\frac{v}{r}\right)^2\right] + \left(\frac{\partial w}{\partial r} + \frac{\partial v}{\partial z}\right)^2\right\} - \rho \epsilon}_{S_\Phi} \tag{18}$$

For the transport equation for ϵ:

$$\frac{\partial}{\partial t}(\rho \epsilon) + \frac{1}{r} \cdot \left[\frac{\partial}{\partial z}(r \rho w \epsilon) + \frac{\partial}{\partial r}(r \rho v \epsilon)\right] - \frac{1}{r} \cdot \left[\frac{\partial}{\partial z}\left(r \cdot \frac{\mu_{\text{eff}}}{\sigma_{\epsilon,\text{eff}}} \cdot \frac{\partial \epsilon}{\partial z}\right)\right] - \frac{1}{r}\left[\frac{\partial}{\partial r}\left(r \cdot \frac{\mu_{\text{eff}}}{\sigma_{\epsilon,\text{eff}}} \cdot \frac{\partial \epsilon}{\partial r}\right)\right] = \underbrace{\frac{\epsilon C_1 \mu_t}{k} \cdot \left\{2\left[\left(\frac{\partial w}{\partial z}\right)^2 + \left(\frac{\partial v}{\partial r}\right)^2 + \left(\frac{v}{r}\right)^2\right] + \left(\frac{\partial w}{\partial r} + \frac{\partial v}{\partial z}\right)^2\right\} - \frac{C_2 \rho \epsilon^2}{k}}_{S_\Phi} \tag{19}$$

For turbulent flow the laminar viscosity, μ_L, is replaced by an effective viscosity, μ_{eff}, given by:

$$\mu_{\text{eff}} = \mu_L + \mu_t \tag{20}$$

The turbulence viscosity, μ_t, described by the turbulence energy k and its dissipation rate ϵ, is given by:

$$\mu_t = C_D \rho k^2/\epsilon \tag{21}$$

where C_D is a constant. $\sigma_{\kappa,\text{eff}}$ and $\sigma_{\epsilon,\text{eff}}$ take the place of a "Prandtl number" for κ and ϵ, respectively. This turbulence model includes five empirical constants with their recommended values being $C_D = 0.09$; $C_1 = 1.43$; $C_2 = 1.92$; $\sigma_k = 1.0$; $\sigma_\epsilon = 1.3$ (Markatos and Moult, 1979).

General differential equation

The above set of Eqs. 2, 3, 4, 11, 14, 15, 18 and 19 may be expressed into the following single form:

$$\underbrace{\frac{\partial}{\partial t}(\rho \cdot \Phi)}_{\text{transient}} + \underbrace{\text{div}\left\{(\rho \vec{v}\Phi}_{\text{convection}} - \underbrace{\Gamma_\Phi \text{grad}\Phi)\right\}}_{\text{diffusion}} = \underbrace{S_\Phi}_{\text{source}} \tag{22}$$

This is the conservation equation for the transport property Φ, where ρ, $\vec{v}$, Γ_Φ and S_Φ are density, velocity vector, effective exchange coefficient of Φ and source rate of Φ per unit volume, respectively (Markatos and Kirkcaldy, 1983). The expressions for Γ_Φ, S_Φ for the variables Φ considered in this work are summarized in Table 2.

Auxiliary Equations and Conditions

The above equation set has to be solved in conjunction with the following auxiliary equations and conditions:

- The density of the particulate phase is constant; for the gaseous phase, the ideal gas assumption is used (Chihara et al., 1978).
- The fluid-to-wall frictional force per unit volume is calculated by:

$$F_\Phi = 1/2 f \rho v^2 A_w \tag{23}$$

where f is the friction factor, ρ and v are the density and velocity of the gas phase and A_w is the contact area per unit volume. The friction factor f is calculated from the log-law wall functions (Launder and Spalding, 1979).

- The momentum loss at perforated screens is calculated by:

$$S_\Phi = 1/2 \rho v^2 f A_w \tag{24}$$

where f is the loss coefficient, and v is the velocity of the gas phase.

- The momentum loss in the packed bed is calculated by the Ergun equation (Froment and Bischoff, 1979).
- The momentum loss at the surfaces of the vessel and at other solid pieces is calculated by:

$$S_{\Phi,P} = 0.0015 \rho v^2 \tag{25}$$

- The temperature differences for the phase in question are calculated from the enthalpy differences by:

$$\Delta h = C_p \Delta T \tag{26}$$

Table 2. Source Terms in Differential Equations

Equations	Φ	S_Φ	Γ_Φ
Continuity	1	0	μ_{eff}
z momentum	w	$-\frac{\partial p}{\partial z} + \frac{\partial}{\partial z}\left(\mu_{\text{eff}} \frac{\partial w}{\partial z}\right) + \frac{1}{r}\frac{\partial}{\partial r}\left(r\mu_{\text{eff}} \frac{\partial v}{\partial z}\right) - F_w - S_{w,P} - S_w - S_{\text{Ergun},w}$	μ_{eff}
r momentum	v	$-\frac{\partial p}{\partial r} + \frac{\partial}{\partial z}\left(\mu_{\text{eff}} \frac{\partial w}{\partial r}\right) + \frac{1}{r}\frac{\partial}{\partial r}\left(r\mu_{\text{eff}} \frac{\partial v}{\partial r}\right) - \frac{2\mu_{\text{eff}} v}{r^2} - F_v - S_{v,P} - S_v - S_{\text{Ergun},v}$	μ_{eff}
Gas-phase mass	C_g	$3 \cdot \rho_f \cdot (1-\epsilon_f) \cdot \frac{k_f}{\epsilon_f r_p} \cdot (C_p\|_{r=r_p} - C_g)$	$\mu_{\text{eff}}/\sigma_g$
Particle-phase mass	C_s	$\{k_i (D_{\text{pore},i})\} \cdot \alpha_f \cdot \psi_p \cdot (C_p - C_s)$	$\mu_{\text{eff}}/\sigma_p$
Gas-phase energy	T_g	$\left(\frac{1-\epsilon}{\epsilon}\right) \cdot \frac{3h}{r_p} \cdot (T_g - T_s\|_{r=r_p})$	$\mu_{\text{eff}}/\sigma_T$
Particle-phase energy	T_s	$h \cdot \frac{6(1-\epsilon_p)}{d_p} \cdot (T_g - T_s) + k_i \cdot \lambda_{\text{ad}} \cdot (C_p - C_s)$	$\mu_{\text{eff}}/\sigma_{Tp}$
Turbulence energy	k	$G_k - \rho \cdot \epsilon$	$\mu_{\text{eff}}/\sigma_{k,\text{eff}}$
Energy dissipation rate	ϵ	$(C_1 \cdot G_k - C_2 \cdot \rho \cdot \epsilon) \cdot \frac{\epsilon}{\kappa}$	$\mu_{\text{eff}}/\sigma_{\epsilon,\text{eff}}$

The above expressions are well-established in literature and appear to respond well to reality.

Solution Method

A finite-domain technique is used, which combines features of the methods of Patankar and Spalding (1972) and a whole-field pressure-correction solver. The space dimensions (and time for transient cases) are discretized into finite intervals, and the variables are computed at only the finite number of locations at the so-called "grid points" (Figure 1). These variables are connected with each other by algebraic equations (finite-domain equations) derived from their differential counterparts by integration over the control volumes or cells defined by the above intervals. This integration leads to equations of the form:

$$\sum_n (A_n^\Phi + \mathrm{Co})\Phi_P = \sum_n A_n^\Phi \Phi_n + \mathrm{Co}\cdot\mathrm{Val} \qquad (27)$$

where the summation n is over the cells adjacent to a defined point P. The coefficients A_n^Φ, which account for convective and diffusive fluxes across the elemental cell, are formulated using upwind differencing. The source terms are written in the linear form $S_\Phi = \mathrm{Co}(\mathrm{Val}-\Phi)$, where Co and Val stand for a coefficient and a value for the variable Φ. A pressure-correction equation is deduced from the finite-domain form of the continuity equation (Patankar, 1980).

The "SIMPLEST" practice of Spalding (1980) is followed, in which the finite-domain coefficients of the momentum equations contain only diffusion contributions with the convection terms being added to the linearized source term. Upwind differencing for convection and harmonic averaging for diffusion are used.

The finite-domain equations for the dependent variables, w, h, and C are solved using a slab-wise simultaneous linear solver

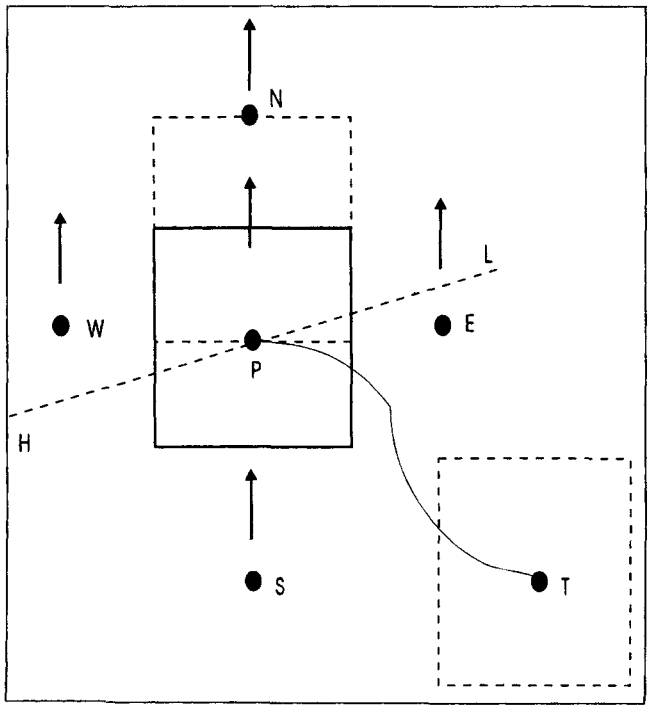

Figure 1. Grid node notation for Eq. 27.

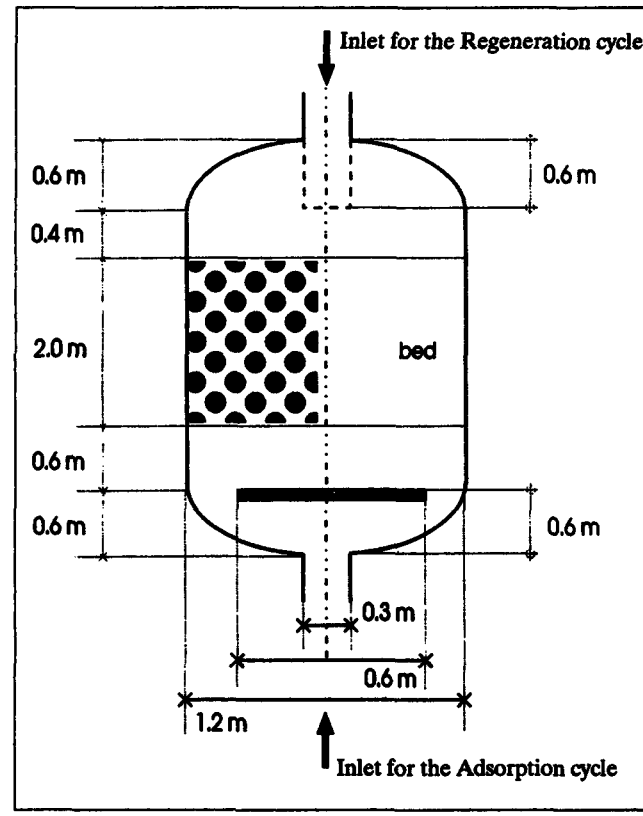

Figure 2. Geometry of the adsorber/regenerator.

(Markatos, 1989). The Jacobi point-by-point linear solver was used for the lateral velocity component v, and a whole-field simultaneous solver was used for the pressure-correction equation. Information about the linear solvers used is provided in Markatos (1989).

The solution procedure is incorporated into a general computer program for the solution of multidimensional and multiphase problems, which has been described elsewhere (Spalding, 1981; Markatos et al., 1982; Markatos, 1983; Theologos and Markatos, 1992).

Results and Discussion

Physical cases considered

The above model was applied to predict the fluid flow and heat/mass transfer in a typical industrial adsorber/regenerator. The geometry of the vessel containing the packed bed is outlined in Figure 2. The packed bed itself is made up of molecular sieve beads, approximately spherical in shape and with a size distribution of between 1.2 mm and 5 mm in diameter. The vessel is cylindrical and axisymmetric.

During the adsorption stage, air enters the vessel through the lower inlet and leaves via the upper pipe. Flow is reversed for the regeneration stage. Two cases were studied, namely mass transfer during the adsorption stage (Case i) and heat/mass transfer during the regeneration stage. Some of the adsorbate properties and other conditions used for the computer simulations are given in Table 3.

Computational details

An iterative procedure is used to solve the discretized dif-

Table 3. Properties and Other Conditions Used in Adsorption/Regeneration Cycle

Properties and Conditions	Adsorption Cycle	Regeneration Cycle
System	*Gas-Particles*	
Inlet Temp., K	293.15	568.15
Inlet Press., bar	6.55	1.2
Avg. Mol. Wt.	28.96	
Bed Void	0.44	
Particles	*Molecular Sieving Carbon*	
Shape	Spherical	
Avg. Size of Particles, mm	d_p (diameter) = 3.9	
Particle Void Fraction - ϵ_p	0.60	
Density of Particles, kg/m^3	$\rho_p = 660$	
True Density of Particles, kg/m^3	$\rho = 1{,}800$	
Specific Heat of the Beads, J/kg·°C	920	
Molec. Diffusivity-D_f, m^2/s	$D_f = 3.86672 \times 10^{-6}$	

ferential equations. Convergence is monitored by the variation between iterations of the field values of the dependent variables. An additional test on convergence is made by computing the sum of the absolute values of the residual sources of the dependent variables. When the magnitudes of these sources have fallen below specified limits, convergence is assumed to have been achieved. For the cases considered here, no problems were encountered in obtaining convergence.

The results were found to be virtually grid-independent for a grid of 40×60. The calculations were performed on an IBM PC-80486 personal computer running under MS-DOS. The number of sweeps of the computational domain required to achieve a prescribed level of convergence for the two cases, along with the time taken for each case are presented in Table 4. It is obvious that predictions of great value for the engineer can be obtained on inexpensive computers with a small expense of time.

Presentation and discussion of results

From the many results obtained, only a few are presented below due to space restrictions.

Case i: Mass Transfer in Packed-Bed, Adsorption Cycle. The present mathematical model is used to predict the rate of adsorption of the solute from the gas phase to the solid-adsorbent.

For comparison purposes, a general theoretical equilibrium isotherm (the Freundlich isotherm) for the adsorption of solutes by adsorbents is shown in Figure 3, with the fitted parameters given in Table 5, as taken from literature (Chihara et al., 1978).

Computed results are presented using plots generated by a graphics package. Flow-field vectors are shown in Figure 4. Peak velocities appear near the axis at inlet and outlet. This is due to the cylindrical geometry and the location of the inlet

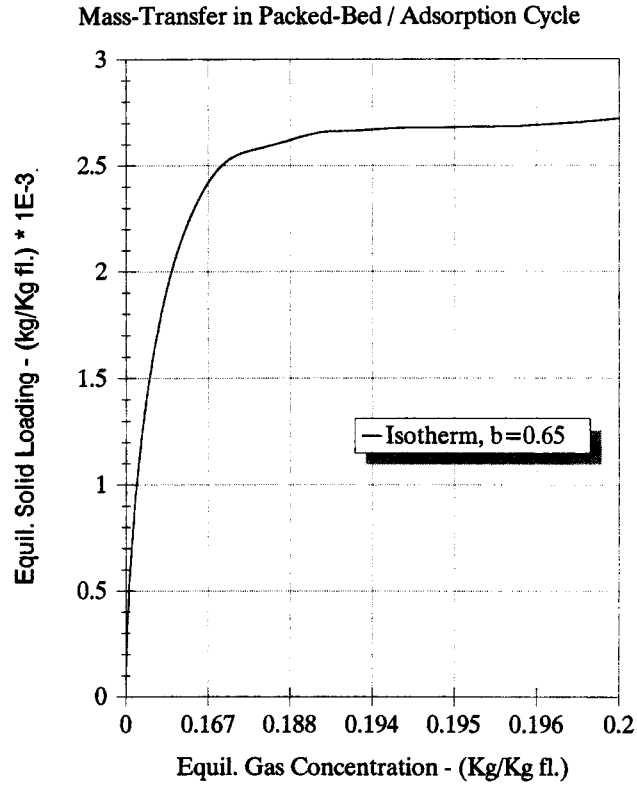

Figure 3. Freundlich isotherm.

and outlet streams. A large recirculation zone driven by the incoming air is observed. The direction of the recirculation is, however, reversed by moving the baffle nearer to the bed. In the bed itself, the flow is evenly distributed with a reduced velocity. On the exit from the bed the flow progresses smoothly past the flow distributor and subsequently out of the flow domain. These are results important to the designer of the

Table 4. Number of Sweeps of the Computational Domain Required to Achieve Given Level of Convergence

	Time Dependency	Grid	Sweeps	Machine-Clock time (s)
Adsorption	Yes	40×60	500/time step	23,709
Regeneration	Yes	40×60	500/time step	23,800

Table 5. Freundlich Isotherms Parameters

T(K)	K	β
293	0.00866	0.65
298	0.00773	0.65
300	0.00740	0.65

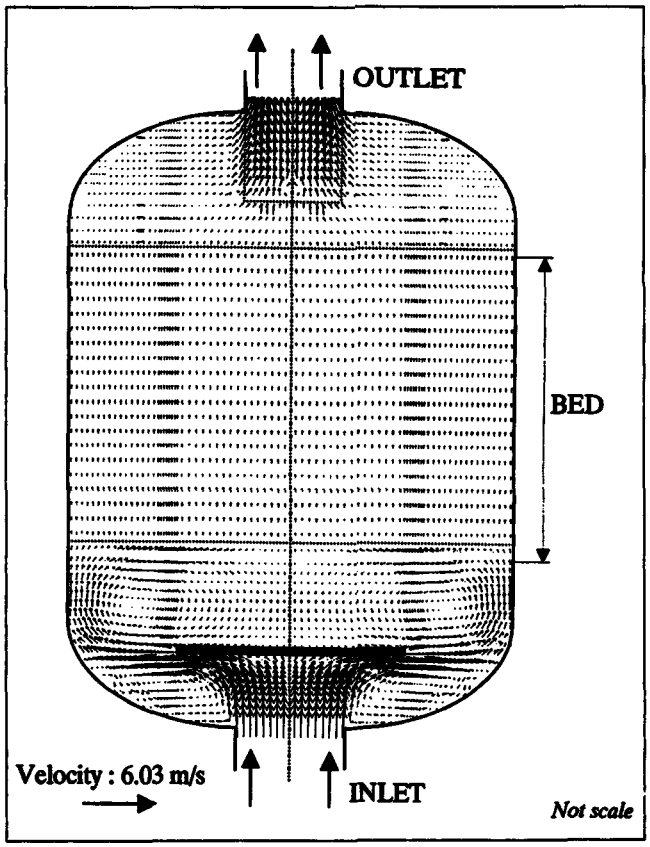

Figure 4. Velocity vectors into adsorption cycle.

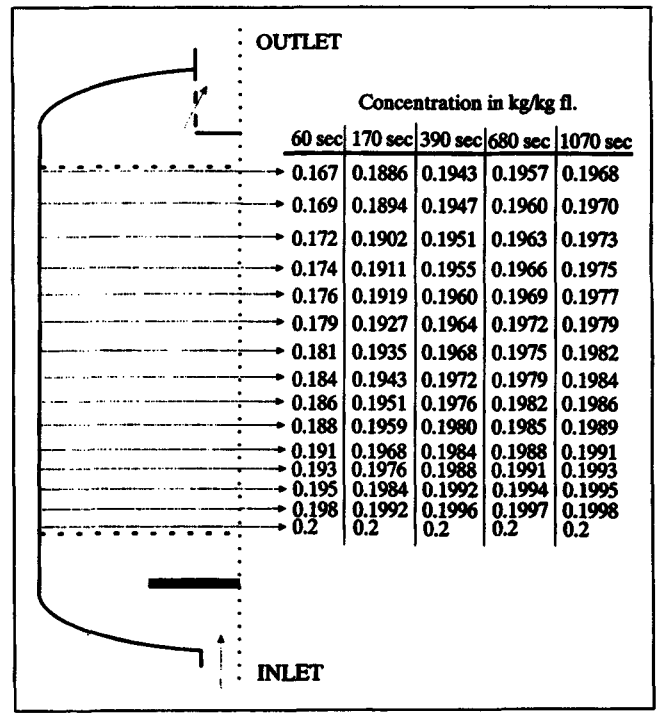

Figure 5. Gas-phase concentration contours during the first 1,070 s into adsorption cycle.

vessel who can thus optimize the hardware according to his specific requirements.

Results for the mass transfer in the adsorption cycle are shown in condensed form in Figures 5 and 6. The length of the column in which sorption uptake is occurring is called the *exchange zone*. The bottom part of this zone is saturated and the top part is fresh. Figure 5 shows the corresponding sorbate concentration profile, also called the wave front, for the exchange zone. The concentration profile is designated as a function, $C_p(Z)_t$, in which Z is distance from the bottom of the column, and t is elapsed time. This profile moves up the column as the sorbent at the bottom of the exchange column becomes saturated (that is, $C_p(Z)_t$ changes as t increases). The $C_p(Z)_t$ function is a solution sought in the modeling process. The complementary solution is the breakthrough curve, designated $C_p(t)_z$. The latter is merely a trace of the concentration profile as it emerges from the end of the column. The pollutant adsorption rate or breakthrough curve is plotted in Figure 6. To the authors' best knowledge, it is the first time that such curves are computed by a general procedure that also predicts full flow and concentration fields.

It is of interest to mention that: the method has been applied for a single-component system, but it is general and can be applied for any multicomponent system, for any geometry of the industrial unit and for any particle-size distribution in the fixed solid phase.

Case II: Heat and Mass transfer in Packed-Bed, Regeneration Cycle. Computed results for Case II are displayed in Figures 7 to 12. Figure 7a shows the flow field, 57 min 50 s, after the start of the regeneration. Figure 7b shows the flow field, 150 min 30 s after the start of the regeneration and 57 min 50 s after the switch from an inlet air temperature of 295°C to 10°C.

It is seen that density variations in the air have a significant effect on the flow field. The gaseous stream entering the bed

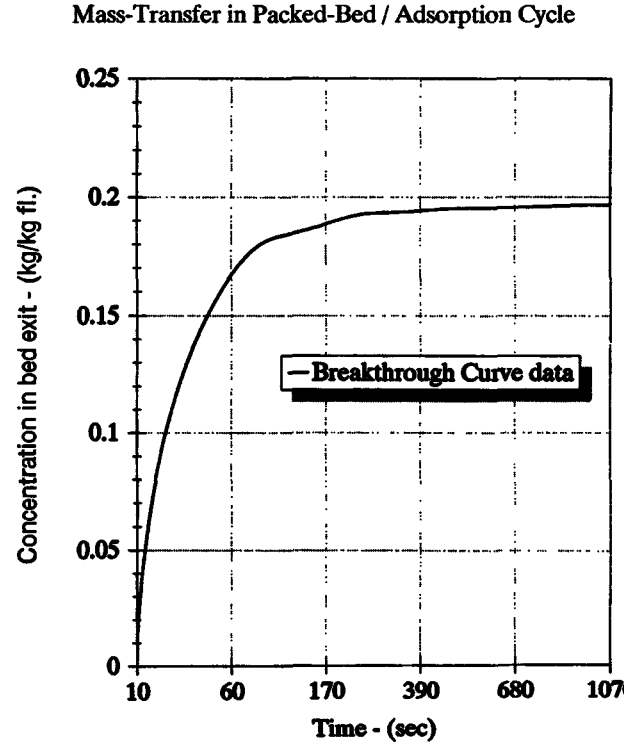

Figure 6. Breakthrough curve.

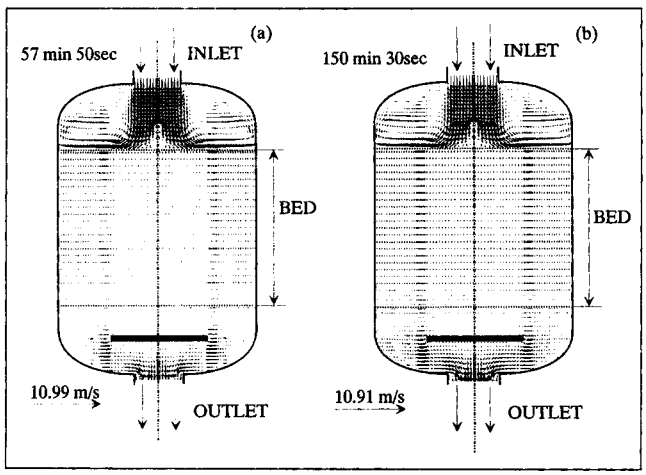

Figure 7. Velocity vectors into regeneration cycle.

for instance slows down in Figure 7a while in Figure 7b there is an increase in speed as expected, since the air is heated up by the bed.

Pressure drop through the bed is plotted in Figure 8. The pressure gradient in the bed is no longer linear due to the temperature gradients (and therefore the density gradients) occurring in the bed.

The temperature field in the packed-bed vessel is shown in Figures 9 to 11. Although in all plots air temperature is shown, the temperatures of the air and the bed are closely tied together, owing to the high density of the bed and the high surface area

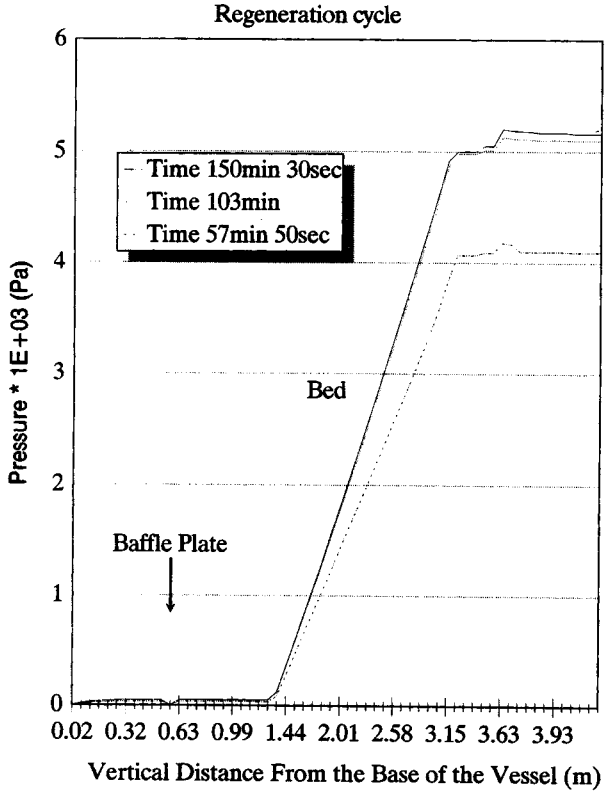

Figure 8. Pressure profiles for the regeneration cycle predictions showing change with time.

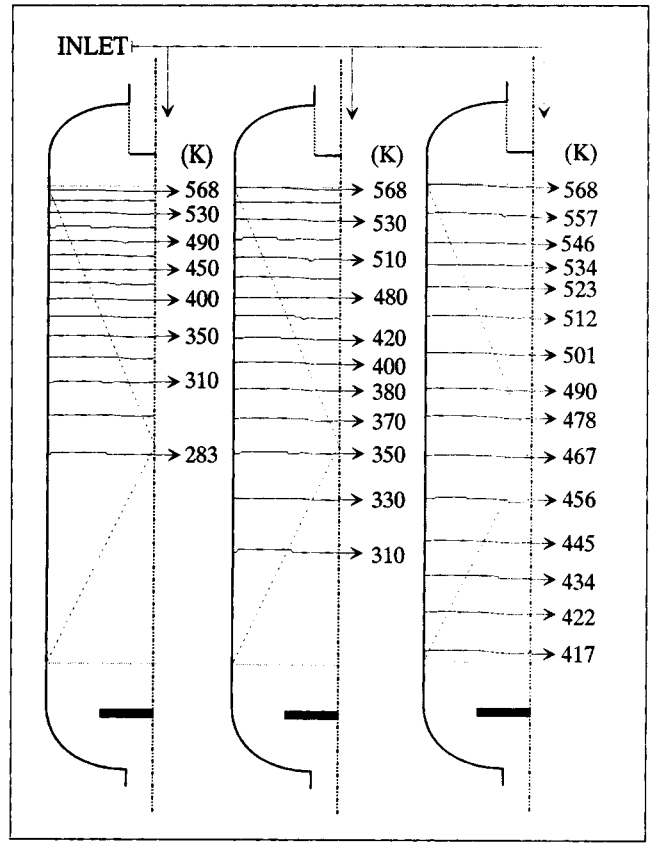

Figure 9. Temperature contours in the vessel during the first 150 min 30 s into regeneration cycle.

represented by the beads for heat transfer. Air temperature, therefore, effectively represents bed temperature in the region of the packed bed.

Figure 9 shows the temperature field over the whole vessel. Contours are shown from 283.15 K to 568 K. The horizontal appearance of each contour demonstrates that progression of the thermal wave through the bed is effectively uniform.

In Figure 10, the thermal wave may be seen to spread into the bed and ultimately penetrate into its full depth. It must be emphasized that the adsorption process has been included in the mathematical model, and therefore heat-transfer effects due to adsorption are predicted. To the best of our knowledge, it is the first time such calculations are performed.

The temperature history at the bed outlet has been plotted in Figure 11. It is interesting to note that the peak temperature is reached after the inlet gas temperature is changed from 10°C to 296°C. This is due to incomplete heating of the bed in the first phase of regeneration and the subsequent progress of the thermal wave through the bed.

Figure 12 presents as a function of the mass velocity a log-log plot of the volumetric heat-transfer coefficients ($h \cdot \alpha_f$) for the two beds of nominal size shale particles. It is seen that there is almost an order of magnitude difference between the heat-transfer coefficients for the smallest shale pieces (1.2 mm) and the largest (2.6 mm). Although there is more scatter in the results for the smaller sized shale, the flow in this bed was clearly more uniform than that in the bed of larger shale. The solid lines drawn through the data in Figure 12 represent "best

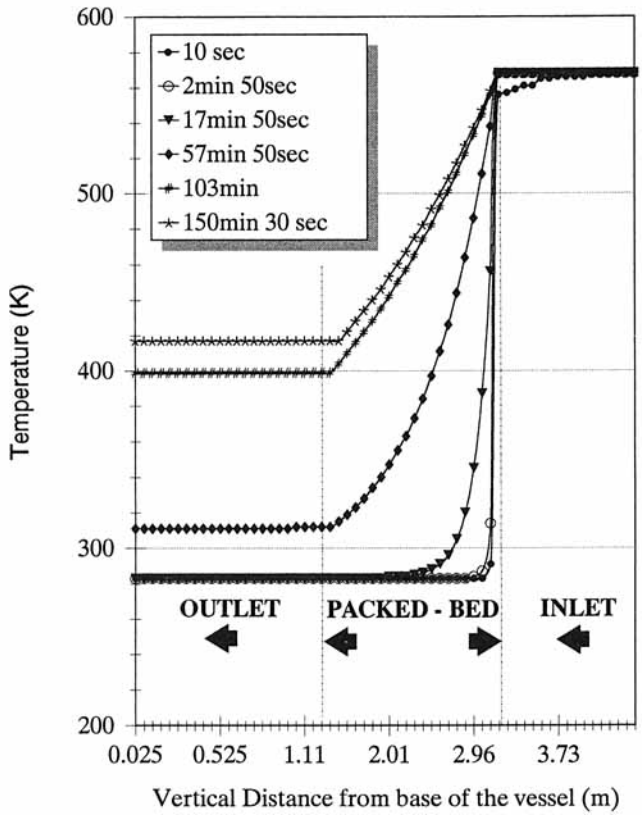

Figure 10. Temperature profiles through the vessel for the regeneration cycle predictions with mass-transfer effects.

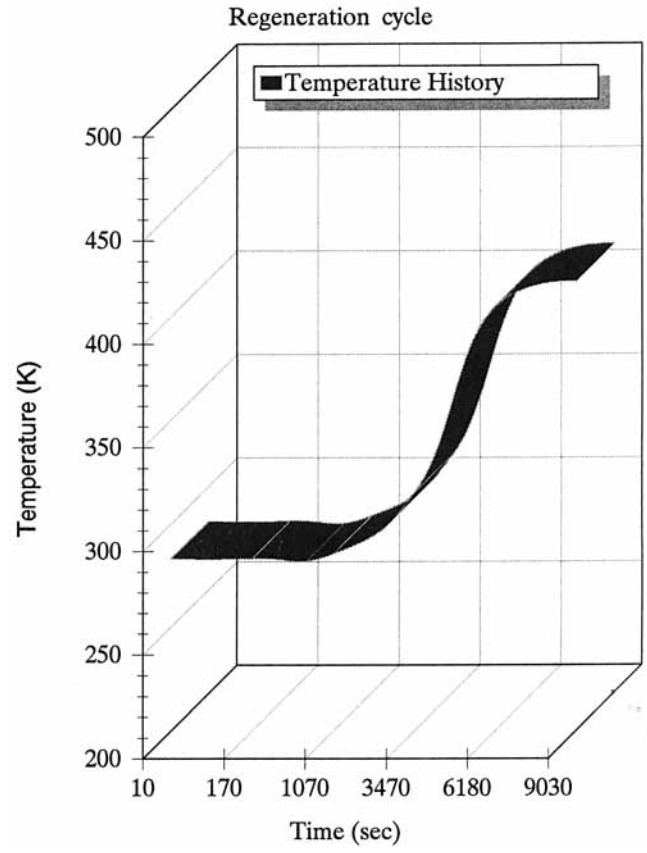

Figure 11. Bed exit temperature as predicted for the regeneration cycle with mass-transfer effects.

fit" lines, and the dependency of $h \cdot \alpha_f$ on velocity is very similar for both beds.

Conclusions

A theoretical model has been developed and used to predict flow, temperature and concentration fields in packed-bed adsorbers/regenerators.

The importance of the proposed approach is that a single and comprehensive model can predict all parameters involved in the design of industrial adsorbers/regenerators, including flow and temperature fields, and can provide fundamental insights and practical responses. For example, effects of gas distribution geometry can be predicted and the relevant results obtained appear physically plausible.

The adsorption system is characterized by a pronounced nonlinearity of the equilibrium curve. A numerical solution of the mathematical model of the nonisothermal one-component adsorption in packed bed was used, including the effect of two intraparticle diffusion mechanisms, mass transfer in the gas film around the particle and diffusion into the porous particle.

It is concluded that physically plausible results may be obtained with the present model for complex engineering processes and equipments, within practical computer resources. More work is required to validate the model against experimental measurements and the performance of real adsorbers, under a variety of operating conditions, and to obtain more reliable experimental correlations for the interphase heat-, mass-, and momentum-transfer, which can then be used to improve the input of the model.

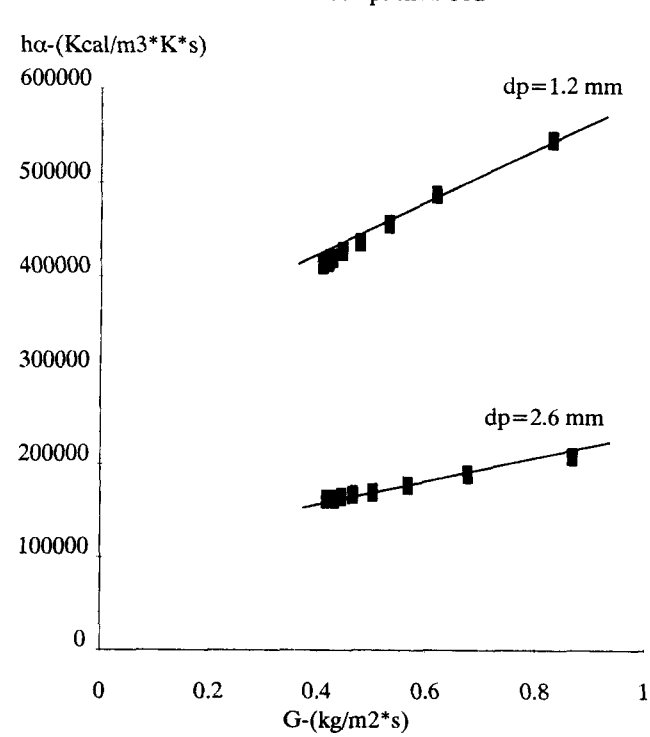

Figure 12. Heat-transfer coefficients-uniform shape beads.

Acknowledgments

The authors wish to thank CHAM Ltd. of London for permitting the use of their general code, PHOENICS. They also thank the E.E.C., DGXII for providing partial funding for this work within the JOULE program.

Notation

A_n^{Φ} = convection-diffusion coefficient in general finite-difference equation
A_w = contact area per unit volume
C_1, C_2, C_D = turbulence model constants
C_g = adsorbate concentration in the gas phase
C_p = concentration of adsorbate at the surface of a pellet
C_s = concentration of adsorbate inside the pellet
d_p = particle diameter
$D_{AB,0}$ = gas-phase diffusivity at 273 K and 1 atm
D_{eff} = effective diffusivity in the gas-phase
f = friction factor
G = mass-flow superficial velocity
h = local heat-transfer coefficient
j_D, j_h = Colburn and Chilton mass- and heat-transfer factor
k = turbulence kinetic energy
k_f = mass-transfer coefficient
N_{Re} = Reynolds number
N_{sc} = Schmidt number of the flowing gas
P = pressure
Pr = air Prandtl number
r_p = particle radius
S_{Φ} = source term of variable Φ in finite-difference equation
t = time
T = general symbol denoting temperature
v, w = radial and axial velocity, respectively
V = bed volume

Greek letters

α_f = specific surface per unit volume of adsorber particle
Γ_{Φ} = symbol denoting the exchange coefficient for dependent variable Φ
ϵ = dissipation rate of turbulence kinetic energy
ϵ_f = void volume fraction in the adsorber (bed)
μ_{eff} = effective viscosity
ρ_f = fluid density
$\sigma_{\Phi,\text{eff}}$ = effective Prandtl/Schmidt number for transport of dependent variable Φ
φ = shape factor
Φ = general symbol denoting a dependent variable

Literature Cited

Carter, J. W., "A Numerical Method for Prediction of Adiabatic Adsorption in Fixed Beds," *Trans. Inst. Chem. Eng.*, **44**, 253 (1966).
Chihara, K., M. Suzuki, and K. Kawazoe, "Adsorption Rate on Molecular Sieving Carbon by Chromatography," *AIChE J.*, **24**(2), 237 (1978).
Dwivedi, P. N., and S. N. Upadhyay, "Particle-Fluid Mass Transfer in Fixed and Fluidized Beds," *Ind. Eng. Chem. Process Dev.*, **16**(2), 157 (1977).
Froment, G. F., and K. B. Bischoff, *Chemical Reactor Analysis and Design*, Wiley, New York, p. 475 (1979).
Hougen, O. A., *Chemical Process Principles*, Part III, Wiley, New York (1948).
Harlow, F. H., and P. I. Nakayama, *Transport of Turbulence Decay Rate*, LA-3854 Los Alamos Science Lab., Univ. of California (1968).
Kyte, W. S., "Nonlinear Adsorption in Fixed Beds: the Freundlich Isotherm," *Chem. Eng. Sci.*, **28**, 1853 (1973).
Launder, B. E., and D. B. Spalding, "The Numerical Computation of Turbulent Flow," *Comp. Meths. Appl. Mech. Eng.*, Vol. 3, 269 (1974).
Marcussen, L., "Comparison of Experimental and Predicted Breakthrough Curves for Adiabatic Adsorption in Fixed Bed," *Chem. Eng. Sci.*, **37**, 299 (1982).
Markatos, N. C., "Computer Simulation of Turbulent Fluid Flow in Chemical Reactors," *Adv. Eng. Software*, **5**(1), 32 (1983).
Markatos, N. C., "Computational Fluid Flow Capabilities and Software," *Ironmaking and Steelmaking*, **16**(4), 266 (1989).
Markatos, N. C., and D. Kirkcaldy, "Analysis and Computation of Three-Dimensional Transient Flow and Combustion Through Granulated Propellants," *Int. J. Heat Mass Transfer*, **26**, 1037 (1983).
Markatos, N. C., and A. Moult, "The Computation of Steady and Unsteady Turbulent, Chemically-Reacting Flows in Axisymmetrical Domains," *Trans. Inst. Chem. Eng.*, **57**, 156 (1979).
Markatos, N. C., N. Rhodes, and D. G. Tatchell, "A General Purpose Program for the Analysis of Fluid Flow Problems," *Numerical Methods for Fluid Dynamics*, Academic Press, New York, p. 463 (1982).
Mckay, G., "Mass Transfer Processes During the Adsorption of Solutes in Aqueous Solutions in Batch and Fixed Bed Adsorbers," *Chem. Eng. Res. Des.*, **62**, 235 (1984).
Meyer, O. A., and T. W. Weber, "Nonisothermal Adsorption in Fixed Beds," *AIChE J.*, **13**, 457 (1967).
Patankar, S. V., and D. B. Spalding, "A Calculation Procedure for Heat Mass and Momentum Transfer in Parabolic Flows," *Int. J. Heat Mass Transfer*, **15**, 1787 (1972).
Patankar, S. V., *Numerical Heat Transfer and Fluid Flow*, McGraw-Hill, New York (1980).
Perry, R. H., and C. H. Chilton, *Chemical Engineers' Handbook*, Fifth ed., p. 16.4 (1973).
Pan, C. Y., and D. Basmadjian, "An Analysis of Adiabatic Sorption of Single Solutes in Fixed Beds: Pure Thermal Wave Formation and Its Practical Implications," *Chem. Eng. Sci.*, **25**, 1653 (1970).
Rosen, J. B., "Kinetics of a Fixed Bed System for Solid Diffusion into Spherical Particles," *J. Chem. Phys.*, **20**, 387 (1952).
SeeSee, T. A., and W. J. Thomson, "Gas-Solid Heat Transfer Coefficients in Beds of Crushed Oil Shale," *Ind. Eng. Chem. Process Dev.*, **16**(2), 243 (1977).
Spalding, D. B., "Mathematical Modelling of Fluid Mechanics, Heat Transfer and Chemical-Reaction Processes," Lecture Course, Imperial College, London, CFDU Report No. HTS/80/1 (1980).
Spalding, D. B., "A General Purpose Computer Program for Multi-Dimensional One-and-Two Phase Flow," *Mathematics and Computers in Simulation*, **23**, 267 (1981).
Theologos, K. N., and N. C. Markatos, "Modelling of Flow and Heat Transfer in Fluidized Catalytic-Cracking Riser-Type Reactors," *Trans. Inst. Chem. Eng.*, **70**, Part A, 239 (1992).
Treybal, R. E., *Mass Transfer Operations*, McGraw-Hill, New York (1968).
Upadhyay, S. N., and G. Tripathi, "Mass Transfer in Fixed and Fluidized Beds," *J. of Sci. and Ind. Res.*, **34**(1), 10 (1975).
Weber, T. W., and P. K. Chakravorti, "Pore and Solid Diffusion Models for Fixed-Bed Adsorbers," *AIChE J.*, **20**, 228 (1974).

Manuscript received Dec. 3, 1992, and revision received Mar. 11, 1993.